# An Image Signal Processor for Ultra Small HD-Grade Video Sensor with 3A in Camera Phones

**Won-Woo Jang, Joo-Hyun Kim, Hag-Yong Han, Hoon-Gee Yang and Bong-Soon Kang**, *Member, KIMICS*

***Abstract*—**In this paper, we propose an image signal processor (ISP) for an ultra small HD-grade video sensor with 3A (AWB, AE, and AF) in camera phones that can process 720P/30fps videos. In order to enhance the video quality of the systems, it is necessary to achieve the high performance of the 3A. The proposed AWB algorithm multiplies the adjusted coefficients of color gains to the captured data of white objects. The proposed AE method adopts the index step moving based on the difference between an averaged Y luminance and a target luminance, together with IIR filters with variable time responses. The proposed AF technique controls the focus curve to find the lens position that maximizes the integrated high frequency components in luminance values by using highpass filters. Finally, we compare the image quality captured from our system to the quality of a commercial HD camcorder in order to evaluate the performance of the proposed ISP. The proposed ISP system is also fabricated with 0.18um CMOS flash memory process.

***Index Terms*—** Image signal processor, 3A, AWB, AE, AF, Adaptive Color Samples, Index Step Moving

## I. INTRODUCTION

Recently, advances in digital technology have allowed people to get mobile phones with numerous sophisticated technologies, such as digital cameras, DMBs, MP3s, etc. The camera function plays a very important role in mobile phones nowadays. Because of the popularization of camera phones, consumers are inclined to take photos and video files for their own precious memories. Also, many video files are propagated via UCC community sites. To enhance the quality of the videos (or images) generated by camera phones, it is necessary to implement three basic functions that are auto white balance (AWB), auto exposure (AE), and auto focus (AF) [1-7].

The sunrays, fluorescent and incandescent bulbs can light up white objects; thereby people can see white objects easily [8]. Although observed white objects appear natural under the sunrays, they look bluish under fluorescent bulbs and reddish under incandescent bulbs. The color temperature of a light source can be determined by comparing its chromaticity with a theoretical black-body radiator [9]. Although color temperatures of the sources are varied under different environments, human eyes have the 'color constancy' ability to cope with different lighting conditions by adjusting their spectral responses while video cameras do not [2]. This is why the white object will not look like white through the video devices. A means has to be developed to define the white criterion that can measure the difference between the white object and the captured object [10]. It is called the AWB. Many studies have been conducted for the AWB so far. Among them, the white patch algorithm estimates the white by finding R, G, and B values from input videos [11], the neural networks algorithm obtains the white estimation by using two of neural networks trained differently [12], and the grayworld algorithm determines the averaged gray value from R, G, and B values [13].

The pupil is located in the front-center of a human eye, and it controls the amount of lights passing through the eye by changing its size. In this manner, image capturing devices continually set the mechanical iris and the electronic rolling shutter for the desirable luminance of the image. There are two auto exposure systems applicable to them [3-4]. One is the photometric sensor because the capturing devices having the sensor can measure the precise luminance strength of nearby objects. The strength of faraway objects can not be determined accurately, however.

Manuscript received November 10, 2009 ; revised November 19, 2009.

Won-Woo Jang, Hag-Yong Han, and Bong-Soon Kang are with the Dept. of Electronics Engineering, Dong-A University, Busan 604-714, South Korea (Tel: +82-51-200-7703, Fax: +82-51-200-7712, Email: bongsoon@dau.ac.kr)

Joo-Hyun Kim is with the SAMSUNG Electro-Mechanics Co. Ltd., Suwon 443-743, South Korea

Hoon-Gee Yang is with Dept. of Radio science Engineering, Kwangwoon University, Seoul 139-701, South Korea

The other is the through-the-lens (TTL) system that is employed in most capturing devices. Among many AE algorithms, the AE prediction algorithm is performed based on the image database that includes more than 2000 pictures to find the AE lookup table for normal condition [1], and the backlight detection algorithm can control the exposure time by splitting the image into five windows and applying each different weight value to corresponding windows [2].

The cornea is also located in the front part of the human eye to protect iris, pupil, and anterior chamber, and so on. With the lens in the human eye, the cornea refracts lights into the pupil, and then helps the eye to focus [14-15]. In this manner, image capturing devices continually set the mechanical iris, zoom, and focus in accordance with the characteristics of optical lens positions. There are many researches for the AF so far. The modified fast climbing search algorithm uses the mountain-climbing serve and hill-climbing search to set two areas for an edge point count and an illuminant gradient of an image [1]. The integrated luminance algorithm can generate the focus signals from two windows, and conduct the search mode to decide the initial direction of the lens movement and the watch mode to decide whether the search operation will resume or not [2].

The popular commercial products of digital still cameras and camcorders use micro controller units (MCU) and macro memories to conduct the 3A for capturing images [2, 4, 6-7, 16-17]. It may be difficult to load the camera module with the 3A on a slim mobile phone due to the limitations in manufacturing technologies. This additional requirement also adds extra cost to the camera module. To solve the problem, without MCUs and macro memories, we propose a new ISP for an ultra small HD-grade video sensor with 3A that can implement 720P (1280pixels×720lines×30fps) HD videos. We propose the AWB algorithm that multiplies the adjusted coefficients of color gains to the captured data of the white objects. We use adaptive color samples for adjusting the objects to fourteen different groups. We introduce the AE method that adopts the wide AE step moving and the index step moving based on the difference between the averaged Y luminance and the target luminance to reduce the time responses and exclude possible frame oscillations. We also propose the AF technique to control the focus curve to find the lens position that maximizes the integrated high frequency components in luminance values by using highpass filters.

The paper is organized as follows. In Section II, the proposed 3A algorithms are described. Section III shows the prototype system board and IC chip, and the experimental results are presented in section IV. Finally, we conclude the paper in section V.

## II. Proposed AWB, AE, and AF Algorithms

### *A. Auto White Balance*

AWB is to change the data measured from white objects to 'real' white data since the measurements contain incorrect color information. Firstly, we propose to average the color-difference signals (e.g., CbCr, UV, or IQ), and then determine the color gain of R and B by using the averaged values. We then divide all the pixels into fourteen groups ($i$ = 1…14) by using three comparisons. They are

$$Y_i < Y_{in},\ CbA_i < Cb_{in} < CbB_i,\ CrA_i < Cr_{in} < CrB_i \quad (1)$$

where $Y_{in}$, $Cb_{in}$, and $Cr_{in}$ denote the component values of YCbCr data in each input pixel. $Y_i$ represents the Y threshold value in the $i$-th group. $CbA_i$ and $CbB_i$ represent two Cb threshold values in the $i$-th group. $CrA_i$ and $CrB_i$ represent two Cr threshold values in the $i$-th group. Secondly, we find the adaptive color samples for the white measure in the summated number $SN_k$. For this purpose, we assume that

$$(N_1 + N_2 > N_3 + N_4 + N_5)\ \&\ (N_1 > N_2 + N_3) \quad (2)$$

$$SN_k = \sum_{i=1}^{k} N_i > N_{color} \quad (3)$$

where $N_1$, $N_2$, $N_3$, $N_4$, $N_5$, and $N_i$ denote the number of pixels in the 1, 2, 3, 4, 5 and $i$-th group, respectively. The $k$ value represents the maximum group number of fourteen in this case. $N_{color}$ is set to at least 40 percent of input pixels to guarantee enough samples. In order to find adaptive color samples, we judge a 'special' image by using Eq. (2) as the criterion. When Eq. (2) is met, we judge the input image to be normal. Otherwise the input is assumed to be abnormal. For the normal, we increase the $i$ value from 1 to 14 until $SN_k$ is larger than $N_{color}$ in Eq. (3). For the abnormal, we increase the $i$ value from 2 to 14 until $SN_k$ is larger than $N_{color}$. Thirdly, we define the averaged values of three component signals of YCbCr as

$$\begin{aligned} Y_{ave} &= \frac{1}{SN_k}\sum_{i=1}^{k} TY_i \\ Cb_{ave} &= \frac{1}{SN_k}\sum_{i=1}^{k} TCb_i \\ Cr_{ave} &= \frac{1}{SN_k}\sum_{i=1}^{k} TCr_i \end{aligned} \quad (4)$$

where $Y_{ave}$, $Cb_{ave}$, and $Cr_{ave}$ denote the values, and $TY_i$, $TCb_i$, and $TCr_i$ represent the accumulated values of the YCbCr pixels in the $i$-th group. We use the conversion equations to derive $R_s$, $G_s$, and $B_s$ [18]:

$$\begin{aligned} R_s &= 1.164\times(Y_{ave}-16)+1.596\times(Cr_{ave}-128) \\ G_s &= 1.164\times(Y_{ave}-16)-0.813\times(Cr_{ave}-128)-0.391\times(Cb_{ave}-128) \\ B_s &= 1.164\times(Y_{ave}-16)+2.018\times(Cb_{ave}-128) \end{aligned} \quad (5)$$

We can now calculate the color gains for the AWB. They are

$$R_{gain}=\frac{G_s}{R_s},\ G_{gain}=\frac{G_s}{G_s}=1,\ B_{gain}=\frac{G_s}{B_s} \quad (6)$$

where $R_{gain}$, $G_{gain}$, and $B_{gain}$ represent R, G, and B color gains. Finally, we adjust all the RGB values by multiplying the color gains as in [19]:

$$R_{new}=R_{gain}\times R_{in},\ G_{new}=G_{in},\ B_{new}=B_{gain}\times B_{in} \quad (7)$$

where $R_{in}$, $G_{in}$, and $B_{in}$ denote the input RGB values. $R_{new}$, $G_{new}$, and $B_{new}$ represent new RGB data corrected by using the proposed AWB.

### *B. Auto Exposure*

AE functions as the analog device that controls the electronic rolling shutter and the mechanical iris to capture the scene within a desired exposure time. We propose to adjust the step of a desired exposure time according to the difference between the averaged Y luminance and the target luminance. Here, we use two methods to get the averaged Y luminance. One is that we divide the input image into sixteen regions having different weighting curves as shown in Fig. 1. In most images, there exist subjects for photography in center regions while there are backgrounds in boundary regions. Small lighting sources or moving white/black objects in the boundary regions cause abrupt changes to the averaged Y luminance, so the overall brightness of the images can be oscillating. Through the method to apply each different weight curve to the regions, we can prevent the images from the oscillation. The other is that we select one pixel in each 4×4 pixels to average the Y luminance values through full image to reduce the algorithm complexity. The averaged value is almost equal to that of whole averaging method, so we can reduce the computational complexity for averaging.

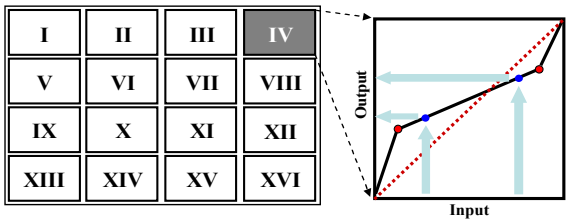


Fig. 1 Sixteen regions and luminance weighting curves

Sudden changes in exposure times may cause the following frame images to flicker. In order to avoid the frame flickers in consecutive frames, we use an IIR filter with variable time responses. The transfer function of the filter is

$$H(z)=\frac{a}{1-(1-a)Z^{-1}} \quad (8)$$

where $a$ indicates a constant value. We can control the exposure time by changing the value of $a$. Figure 2 shows eight time responses of the filter. The fastest and slowest responses are denoted as ⓐ and ⓑ, respectively. ⓐ shows that one frame is required to arrive at 90 percent of the maximum, whereas ⓑ needs 16 frames.

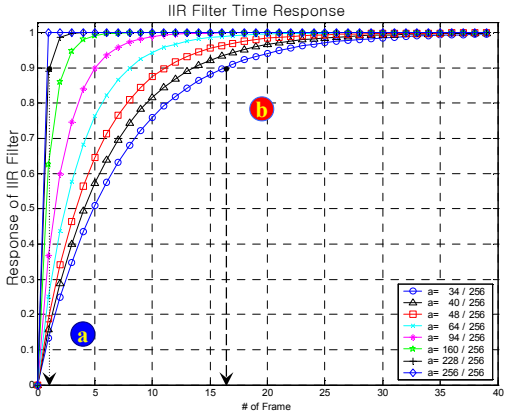


Fig. 2 The time responses of IIR filters

The wide AE step moving is used to move to the target luminance more quickly; however, it causes another image oscillation between adjacent frames of slightly bright and slightly dark. Therefore, we introduce the stabilization method as shown in Fig. 3. When the present AE step is in the IIR filter area, we use the filter output to decide the present moving step. When the present AE step is in the index step moving area, we decrease the present moving step slightly. This is called the index step moving. Figure 3-(b) shows the wide AE step moving without the index step moving. Assume that the target luminance is 100

and the start point is 60, the wide AE step can move to the target luminance in every 15 step. However, the AE step oscillates between 90 and 105, denoted as ③, near the target luminance. Figure 3-(c) shows the AE step moving with the index step moving, while the initial conditions are same to Fig. 3-(b). Inside the index step moving, the AE step increases the present moving step by 5 only, thereby arriving at the target luminance denoted as ⑦. Thus we can get rid of another frame oscillation.

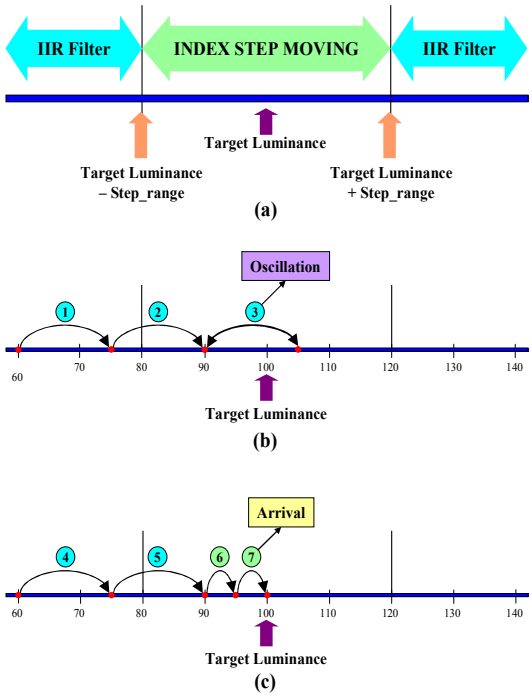


Fig. 3 The diagram of the AE stabilization, (a) the areas of the AE stabilization, (b) the AE step moving without the index step moving, and (c) the AE step moving with the index step moving

*C. Auto Focus*

AF plays an important role in getting clear images of the objects. Because a focused image contains higher frequency components than those of an out-of-focus image [1-3], it is necessary to define a criterion for the focused image. Eq. (9) shows an idea. It is the 15-tap highpass filter that can extract high frequency components in the image. Here, we use Eq. (10) to judge the focused image:

$$H_{AF}(Z) = -(1 + Z^{-1} + Z^{-2} + Z^{-3} + Z^{-4} + Z^{-5} + Z^{-6} - 15Z^{-7} + Z^{-8} + Z^{-9} + Z^{-10} + Z^{-11} + Z^{-12} + Z^{-13} + Z^{-14}) \quad (9)$$

$$AH_{AF} = \sum \left| Y_{in} * H_{AF} \right| \quad (10)$$

where $Y_{in}$ denotes the Y luminance value of the input image and $AH_{AF}$ represents the accumulated absolute value of the high frequency components. We use $AH_{AF}$ to find the focus control value of the fluid lens of the CMOS sensor module. We apply Eqs. (9)-(10) to the same scenes with different lens positions. Figure 4 shows the experimental results. Figures 4-(a), (c), (e), and (g) show the same scenes with different lens position values, and Figs. 4-(b), (d), (f), and (h) show the corresponding extracted edges by using the filter in Eq. (9), respectively. From the extracted edges, we can draw the focus curve as shown in Fig. 5. Figure 5 shows the resulting focus curve based on the different lens positions. From the curve, we can see that the $AH_{AF}$ values are 128,493,652, 153,302,534, 167,710,907, and 136,761,496, respectively. Since the $AH_{AF}$ value peaks when the fluid lens is in focus, Fig. 4-(c) of the (f) position in Fig. 5 reveals the best fit among the four images.

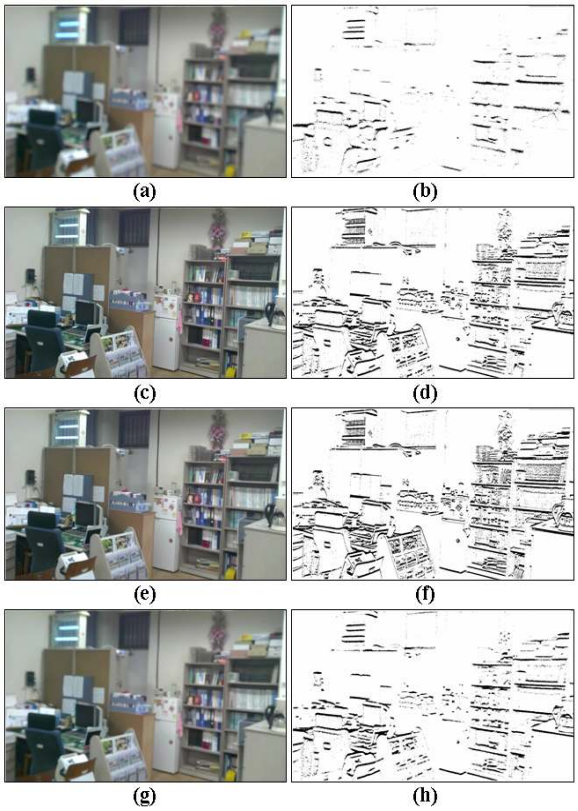


Fig. 4 Same four scenes with different lens position values: (a) No. 87 scene, (b) the edges extracted from (a), (c) No. 112 scene, (d) the edges extracted from (c), (e) No. 121 scene, (f) the edges extracted from (e), (g) No. 137 scene, and (h) the edges extracted from (g)

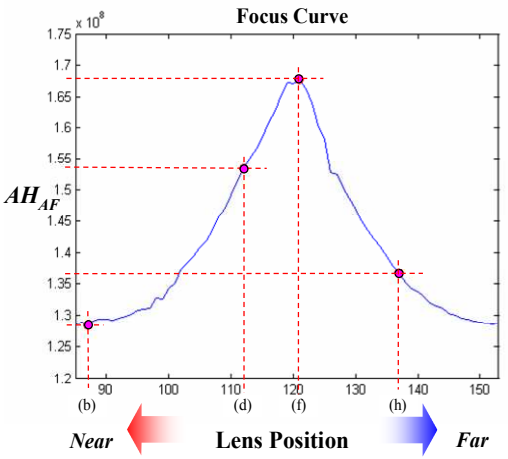


Fig. 5 Focus curve measured from lens position values and component of high frequency signal

We propose AF system with three operational modes: wide search, fine search with hill-climbing algorithm, and watch mode. These are shown in Fig. 6. In the wide search mode, we adjust the focus from a long to a short distance and decide the initial direction of the lens position. In the fine search mode, we use the hill-climbing method for the best lens position to find a possible maximum $AH_{AF}$. In the watch mode, we decide whether the fine search mode will continue or not. To do so, we calculate the absolute difference between the previous maximum $AH_{AF}$ and the present $AH_{AF}$. When the difference is 10 percent bigger, we adjust the lens position to find another maximum $AH_{AF}$. Otherwise, the present position is assumed to produce the focused image. In this manner, we can design the AF system proposed in this paper.

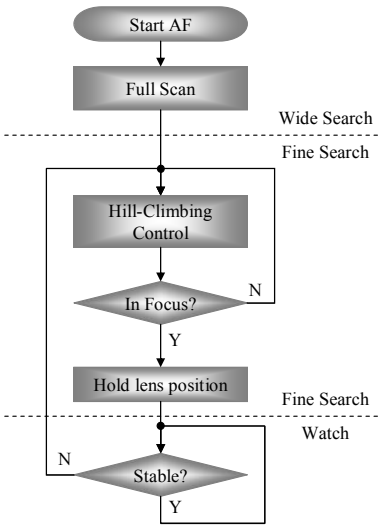


Fig. 6 Flow chart of the proposed AF system

## III. HD Video Camera System

Figure 7 shows the simplified block diagram of the ISP that can be used in mobile applications. The CMOS HD-grade video sensor digitizes data at 60 MHz to meet 720P video out with 10bit A/D converter. The raw data is digitized in the RGB Bayer format through an RGB mosaic color filter array. The AF adjusts the focus of the optical fluid lens through the MCU. The Pre-processing compensates the digitized raw data and derives RGB values from the Bayer signals captured from the CMOS sensor lens. The pre-AWB, together with AWB, calculates new RGB values as shown in Eq. (7). The Color-processing conducts various colors processing such as color matrix, brightness, gamma processing, and so on, and send the processed colors to AE, AF, and Post-processing. The AE also controls the electronic rolling shutter to reach the target luminance value. Post-processing enhances the image quality and sends 16bit 422 YCbCr for the following display devices. We can see that the ISP does not use the MCU to conduct the AE and the AWB.

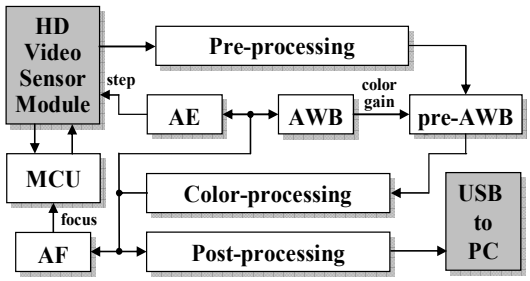


Fig. 7 Simplified block diagram of an image signal processor

Figure 8 shows our prototype HD video camera system. In the middle of the prototype board shown in Fig. 8-(a), we see the ISP chip proposed in this paper. Figure 8-(b) shows the layout of the chip. The chip was designed by using Verilog HDL and fabricated in a 0.18μm CMOS flash memory process. The total gate count is about 1.5M-gates where a 2-input NAND is counted as one gate. The details are given in Table 1.

Table 1 Chip Specifications

| | |
|---|---|
| Technology | 0.18um CMOS flash memory |
| Gate count | 1.5M-gates |
| Clock rate | 60MHz |
| Die size | 5000 mil × 5000 mil |
| Package | 128 pins QFP |

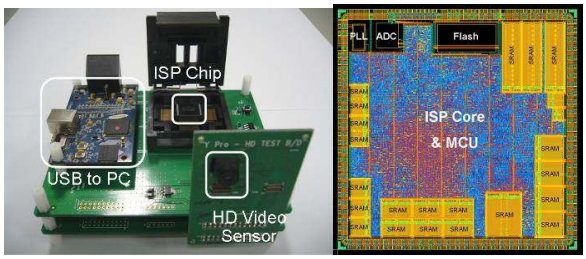


(a) (b)

Fig. 8 Prototype video camera system: (a) prototype HD system and (b) layout of the image signal processor chip

## IV. Simulation and Experimental Results

Figure 9 shows the simulation results of the standard colors archived by the proposed AWB algorithm. The environmental conditions are D65, horizon, and coolwhite. In order to measure the performance of the proposed AWB, we use Euclidean distances ($\Delta E^*_{ab}$) in [20] between the reference white and the white-balanced colors. For an ideal white case, the distance should be zero. From the figures, we can see that the distances for ①, ②, ③, and ④ without AWB in Figs. 9-(a), (c), and (e) are much larger than those with AWB in Figs. 9-(b), (d), and (f), respectively. Because the average of Euclidean distances in the Fig. 9 decreased 67.6 percent, this reveals that the proposed AWB performs very well to achieve the white under the three conditions.

Other experiments are conducted to test the performance of each AE, AWB, and AF proposed in this paper. Figure 10 shows the AWB performance. Once again, we see that the Euclidean distances without AWB in Fig. 10-(a) are larger than those with AWB in Fig. 10-(b), respectively. Figure 11 represents the AE performance. Figure 11-(a) shows the image with normal light source, while Fig. 11-(b) shows the image with extreme light source. We evaluate the performance of AE by repeatedly turning on and off a desk lamp to test the oscillation problem. From the tests, we conclude that the image oscillations are removed with the proposed AE. Figure 12 shows the test results for the proposed AF. Figure 12-(b) shows the focused image obtained from the proposed AF, where Fig 12-(a) shows the blurred image under the out-of-focus condition. From these various tests, we conclude that the system performs very well with the 3A proposed in this paper.

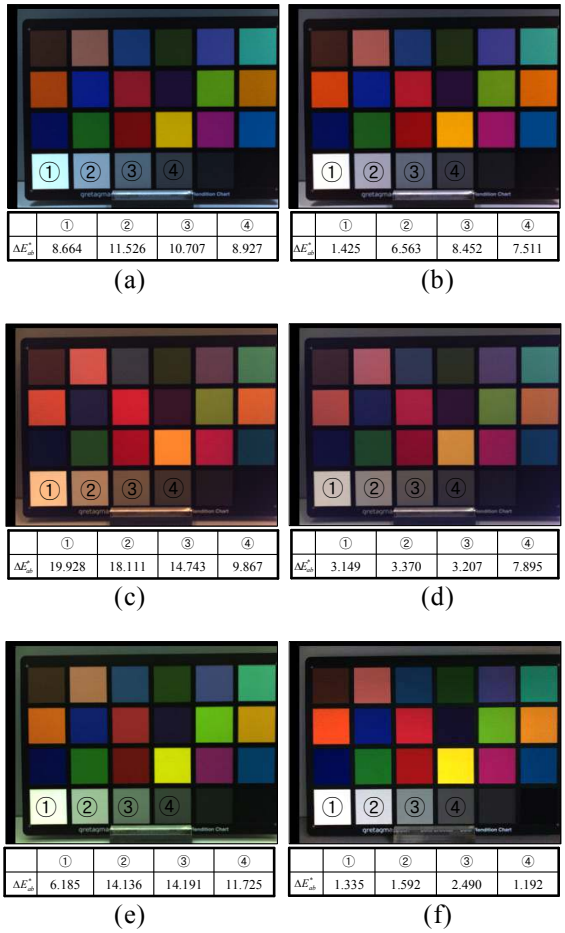


Fig. 9 AWB simulation results: (a) D65 without AWB, (b) D65 with AWB, (c) horizon without AWB, (d) horizon with AWB, (e) coolwhite without AWB, and (f) coolwhite with AWB [9]

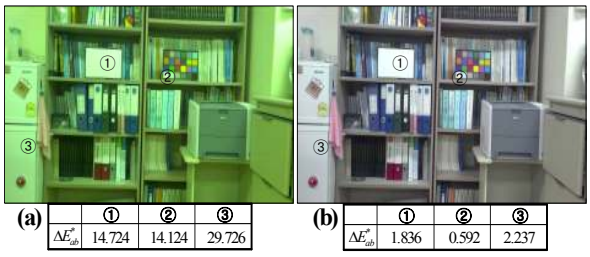


Fig. 10 AWB experimental results: (a) compound image without AWB and (b) compound image with proposed AWB

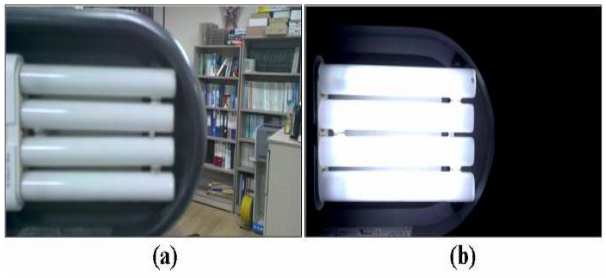

(a) (b)

Fig. 11 AE experimental results: (a) compound image under the normal light source and (b) compound image under the extreme light source

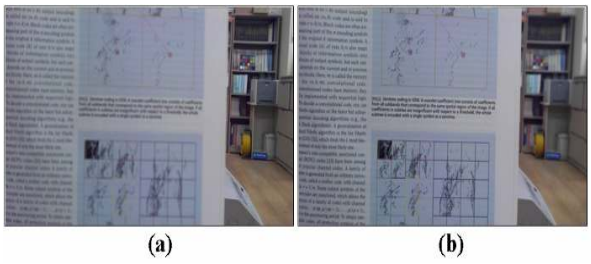

(a) (b)

Fig. 12 AF experimental results: (a) out-of-focused image and (b) focused image

Additional experiments are conducted to see the overall performance of the 3A proposed in this paper. In order to compare the performance of our ISP with a commercial HD camcorder, we set up the illuminance of 700 lux for a strong illumination condition and 20 lux for a weak illumination condition. Figures 13-14 shows the results. Figures 13-(a) and 14-(a) are obtained from the proposed system, and Fig. 13-(b) and 14-(b) are obtained from a commercial HD camcorder, respectively. Compared to Fig. 13-(b), we can see that Fig. 13-(a) has clearer aspects that are the doll, the blue letters on the panel, the red clock and tea utensils. We can also see that Fig. 14-(a) contains less noise in the background and a slightly brighter image than Fig. 14-(b). Although we use a small size lens for slim mobile phones, we see that our ISP with 3A processes HD-grade live videos of 1280pixels× 720lines×30fps

.

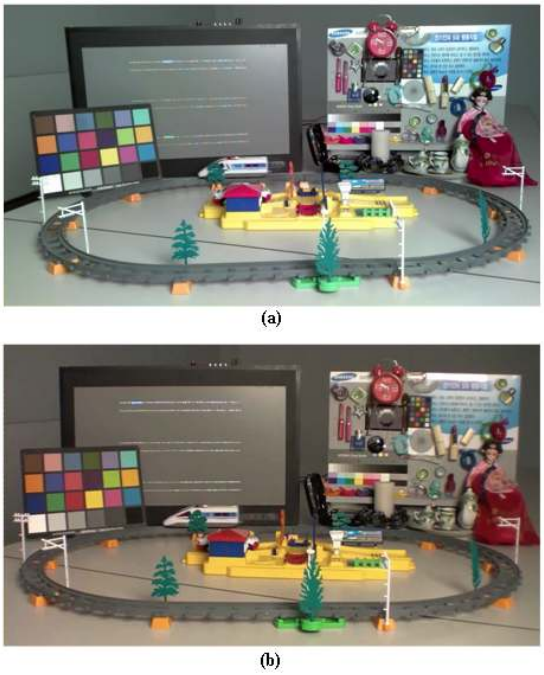

(a)

(b)

Fig. 13 Strong illumination condition: (a) compound image by HD video camera system and (b) compound image by a commercial HD camcorder under the illuminance of 700 lux

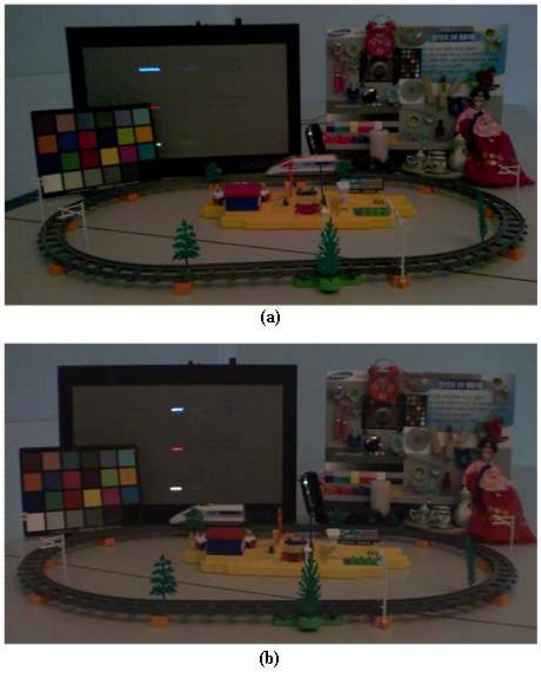

(a)

(b)

Fig.14 Weak illumination condition: (a) compound image by HD video camera system and (b) compound image by a commercial HD camcorder under the illuminance of 20 lux

## IV. Conclusions

In this paper, we presented the ISP with 3A for an ultra small HD-grade video sensor that can be applied to the mobile camera phones. The input image was the videos of 1280pixels×720lines×30fps. The proposed ISP conducted the AE and AWB without MCUs. It did not use bulky or frame memories for these functions. The proposed system reduced the processing times for AWB, AE, and AF to process the HD-grade live videos. Although our ISP is used for a slim mobile phone, our HD video system with the proposed ISP shows the higher quality as compared with that of a commercial HD camcorder. Due to the ability to process the HD-grade live videos, the proposed system may be an attractive IP when combined with other processing units for mobile devices.

## ACKNOWLEDGMENT

This paper was supported by research funds from Dong-A University.

## REFERENCES

[1] W. Kao, S. Chen, T. Sun, T. Chiang, and S. Lin, "An Integrated Software Architecture for Real-Time Video and Audio Recording Systems," IEEE Trans. on Consumer Electronics, Vol. 51, No. 3, pp. 879 – 884, Aug. 2005.

[2] J. Lee, Y. Jung, B. Kim, and S. Ko, "An Advanced Video Camera System with Robust AF, AE, and AWB Control," IEEE Trans. on Consumer Electronics, Vol. 47, No. 3, pp. 694 – 699, Aug. 2001.

[3] S. Sohn, S. Yang, S. Kim, K. Baek, and W. Paik, "SoC Design of An Auto-Focus Driving Image Signal Processor for Mobile Camera Applications," IEEE Trans. on Consumer Electronics, Vol. 52, No. 1, pp. 10 – 16, Feb. 2006.

[4] T. Kuno, H. Sugiura, and N. Matoba, "A new automatic exposure system for digital still cameras," IEEE Trans. on Consumer Electronics, Vol. 44, No. 1, pp, 192 – 199, Feb. 1998

[5] J. He, R. Zhou, and Z. Hong, "Modified Fast Climbing Search Auto-focus Algorithm with Adaptive Step Size Searching Technique for Digital Camera," IEEE Trans. on Consumer Electronics, Vol. 49, No. 2, pp. 257 – 262, May 2003.

[6] A. Morimura et al., "A Digital Video Camera System," IEEE Trans. On Consumer Electronics, Vol. 36, No. 4, pp. 866 – 876, Nov. 1990.

[7] D. Doswald, J. Hafliger, P. Blessing, N. Felber, P. Niederer, and W. Fichtner, "A 30-frames/s megapixel real-time CMOS image processor," IEEE Trans. on Solid-State Circuits, Vol. 35, No. 11, pp. 1732 – 1743, Nov. 2000.

[8] J. Ha, S. Lee, T. Kim, W. Choi, and B. Kang, "A New Approach to Color Adjustment for Mobile Application Display with a Skin Protection Algorithm on a CIE1931 Diagram," IEEE Trans. on Consumer Electronics, Vol. 53, No. 1, pp. 191–196, Feb. 2007.

[9] W. Jang, K. Son, J. Kim, and B. Kang, "Auto White Balance System Using Adaptive Color Samples for Mobile Devices," pp. 1462 – 1465, IEEE APCCAS2008, Dec. 2008.

[10] J. Huo, Y. Chang, J. Wang, and X. Wei, "Robust Automatic White Balance Algorithm using Gray Color Points in Images," IEEE Trans. on Consumer Electronics, Vol. 52, No. 2, pp. 541–546, May 2006.

[11] G. Buchsbaum, "A spatial processor model for object colour perception," Journal of Franklin Institute, Vol.310, No. 1, pp. 1 – 26, 1980.

[12] V. Cardei, B. Funt, and K. Barnard, "Adaptive illuminant estimation using neural network," Proc. Of the 8th Int. Conf. on Artificial Neural Network, pp.749 – 754, Skvde, Sweden, 1998.

[13] E.H. Land, "The retinex theory of color vision," Scientific American, pp. 108-129, 1997.

[14] B. Cassin and S. Solomon, *Dictionary of Eye Terminology*. Gainsville, Florida: Triad Publishing Company, 1990.

[15] E. B. Goldstein, *Sensation & Perception*. 7th Edition. Canada: Thompson Wadsworth, 2007.

[16] H. Yoshida, S. Okada, H. Murata, M. Kurokawa, and H. Okada, "Ultra small HD video camera using MPEG4 codec with SD memory card as storage," ICCE, 8.3-3, Jan. 2007.

[17] S. W. Lee, Y. Kumar, J. M. Cho, S. W. Lee, and S. W. Kim, "Enhanced autofocus algorithm using robust focus measure and fuzzy reasoning," IEEE Trans. On Consumer Electronics, Vol. 18, No. 9, pp. 1237-1246, Sep. 2008.

[18] R. C. Gonzalez, *Digital Image Processing*, 3rd ed., Addison Wesley Longman, 2007.

[19] W. Jang, B. Kwak, J. Kim, and B. Kang, "An Image Signal Processor For Ultra Small HD Video Sensor With 3A In Camera Phones," ICCE, 3.3-3, Jan. 2009.

[20] R. Pete, *Digital Color Correction*, Thomson Learning, 2005.

**Won-Woo Jang**
Member KIMICS. Received the B.S and M.S. degrees in electronics engineering from Dong-A University, Busan, Korea, in 2005 and 2007, respectively. He is currently working toward his Ph.D. degree at the university. His research interests include digital camera processing systems, VLSI architecture design and image processing.

**Joo-Hyun Kim**
Member KIMICS. Received the B.S., M.S. and Ph.D. degrees in electronics engineering from Dong-A University, Busan, Korea, in 2002, 2004 and 2007, respectively. He is now with Samsung Electro-Mechanics Co. Ltd., Suwon, Korea. His research interests include digital camera processing systems, VLSI architecture design and image processing.

**Hag-Yong Han**
Member KIMICS. Received the B.S., M.S. and Ph.D. degrees in electronics engineering from Dong-A University, Busan, Korea, in 1994, 1998 and 2004, respectively. He had worked as Chief of R&D at the Easy Harmony Co. Ltd., Busan, Korea, in 2001, and a post doctoral researcher at the Pusan National University, Busan Korea, in 2006 -2007, respectively. He now is the research professor of the Multimedia Research Center of the Dong-A University. His research interests include pattern recognition, audio / image / video processing, DSP application

**Hoon-Gee Yang**
Member KIMICS. Received the B.S. degree in electronics engineering from Yonsei University, Seoul, Korea, in 1985 and the MS and PhD degrees in electrical and computer engineering from the State University of New York at Buffalo, Amherst, NY, in 1987 and 1992, respectively. From 1993, he has been in the Department of Radio Science and Engineering, Kwangwoon University, Seoul, Korea. His main research interests are the receiver design of the ultrawide-bandwidth communications, array signal processing and the RFID reader/tag design.

**Bong-Soon Kang**
Member KIMICS. Received the B.S. degree in electronics engineering from Yonsei University, Seoul, Korea, in 1985, and the M.S. degree in electrical engineering. from University of Pennsylvania, Pennsylvania, USA, in 1987, and the Ph.D. degree in electrical and computer engineering from Drexel University, Philadelphia, USA, in 1990. From Dec. 1989 to Feb. 1999, he had worked as a senior staff researcher at Samsung Electronics Co. Ltd., Kihung, Korea. Since March 1999, he has been with the department of electronics engineering, Dong-A University, Busan, Korea. He is the director of the Multimedia Research Center of the university. His research interests include image processing, hardware architecture designs, and wireless communications. He was honored as a 2007 winner of the Chester Sall Award for the 1st place best paper in the IEEE Transactions on Consumer Electronics on Jan. 2009.